Strain Analysis in Sandwich Structures using Digital Image Correlation

St. Hartmann, C. Sguazzo

Institute of Applied Mechanics, Clausthal University of Technology

stefan.hartmann@tu-clausthal.de

Abstract

Sandwich structures are composed by different thin-layered materials. One example is a sandwich made of metal - polymer - metal layers, where the internal polymer layer is given by a polypropylene-polyethylene (PP/PE) foil. In experimental observations it turns out that an emerging strain localization requires the entire field information. The application of Digital Image Correlation (DIC) is common in measuring the surface strains of mechanically loaded specimens. However, the literature – both in scientific publications as well as the theory manuals of the providers – leave the question open how the detailed formulation of the strains in the curvilinear setting has to be performed. In this short essay, the fundamentals are discussed, where we draw on surface descriptions developed in the context of finite elements. A second topic treats the strain determination on the surface of finite elements, since for the case of material parameter identification the displacements or even the strains are required for the solution of the entire boundary-value problem. Even here, the strains on the surface of three-dimensional element formulations are not provided by most commercial finite element programs. Thus, the concept of strain determination is transferred to the output of finite element programs as well.

1 Introduction

The development of new constitutive equations requires particular mechanical loading paths applied to specific specimens. In the case of homogeneous deformations (e.g. tension and/or compression) the stress and strain state is constant within a certain region of the specimen so that strain gauges or tension grips are useful. There exist geometries of specimens and specific materials, where an inhomogeneous distribution of strains occurs. In Fig. 1(a) such an example is shown for a PP/PE tensile specimen, in which strains are provided to the user of a DIC-system. However, if one has a closer look at the mathematical formulation, it is hard to find out how strains are determined.

The specimens are sprayed by a dotted lacquer and the DIC-system follows the points, i.e. the system provides coordinates of points either in 2D (one camera) or 3D (two cameras), see, for example, [1]. In the latter reference the procedure to determine some components of the strain tensor is explained in words. Unfortunately, a clear mathematical description in a curvilinear setting is missed so that some interpretation is left to the reader.

Since the strains can only be determined within the specimen's surface – the out-of-plane information cannot be provided – a surface description is required as well. In this respect, we refer to [2, 3, 4]. A further borrowing is made in shell analysis, [5, pp. 320] or [6] and the references cited therein.

The present contribution is organized as follows: first, the theory to determine strains within a curvilinear surface is presented, which is used for the strain determination. Afterwards, the same procedure is applied to determine strains in commercial finite elements.

2 Kinematical Description of Strains

We assume that a curvilinear surface is described by a function of two parameters (surface parameters). A surface in the reference configuration is described by the position vector $\vec{X} = \hat{\vec{X}}(\Theta^1, \Theta^2)$ (given by a surface description), where Θ^1 and Θ^2 describe the surface coordinates, see Fig. 1(b). The quantities $\vec{A}_\alpha = \hat{\vec{X}}_{,\alpha} = \partial\hat{\vec{X}}/\partial\Theta^\alpha$, $\alpha = 1, 2$ are the tangent

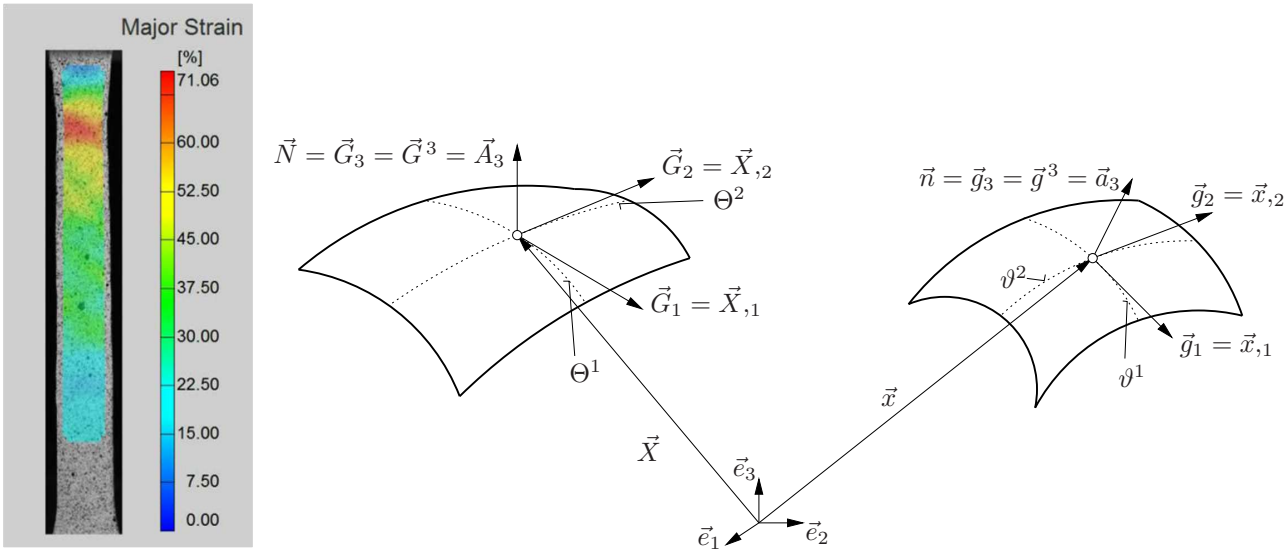

(a) Strain measurement

(b) Kinematical description of the deformation

Figure 1: Surface deformation and its geometrical quantities

vectors and $\vec{A}^\alpha = A^{\alpha\beta}\vec{A}_\beta$ the gradient vectors. $[A^{\alpha\beta}] = [A_{\alpha\beta}]^{-1}$ (with $A_{\alpha\beta} = \vec{A}_\alpha \cdot \vec{A}_\beta$) are the contravariant metric coefficients. In the current configuration we have the coordinates ϑ^1 and ϑ^2, which are described by the motion $\vartheta^\alpha = \theta^\alpha_{\mathrm{R}}(\Theta^\beta)$, $\alpha = 1, 2$, $\beta = 1, 2$. Using the differential

$$\mathrm{d}\vartheta^\alpha = \frac{\partial\theta^\alpha_{\mathrm{R}}}{\partial\Theta^\beta}\mathrm{d}\Theta^\beta \tag{1}$$

we define the material line element in tangential surface of the current configuration by multiplying expression (1) with the spatial tangent vector $\vec{a}_\alpha = \hat{\vec{x}}_{,\alpha} = \partial\hat{\vec{x}}/\partial\vartheta^\alpha$,

$$\mathrm{d}\hat{\vec{x}} = \mathrm{d}\vartheta^\alpha\vec{a}_\alpha = \frac{\partial\theta^\alpha_{\mathrm{R}}}{\partial\Theta^\beta}\mathrm{d}\Theta^\beta\vec{a}_\alpha = \frac{\partial\theta^\alpha_{\mathrm{R}}}{\partial\Theta^\beta}\mathrm{d}\Theta^\gamma \underbrace{\delta_\gamma^{\ \beta}}_{\vec{A}_\gamma\cdot\vec{A}^\beta}\vec{a}_\alpha = \frac{\partial\theta^\alpha_{\mathrm{R}}}{\partial\Theta^\beta}(\vec{a}_\alpha\otimes\vec{A}^\beta)\underbrace{\mathrm{d}\Theta^\gamma\vec{A}_\gamma}_{\mathrm{d}\vec{X}} = \hat{\mathbf{F}}\mathrm{d}\hat{\vec{X}}. \tag{2}$$

The singular tensor

$$\hat{\mathbf{F}} = \frac{\partial \theta_{\mathrm{R}}^{\alpha}}{\partial \Theta^{\beta}} (\vec{a}_{\alpha} \otimes \vec{A}^{\beta}) = \theta_{\mathrm{R},\beta}^{\alpha} \, (\vec{a}_{\alpha} \otimes \vec{A}^{\beta}) \tag{3}$$

is interpreted as the in-plane deformation gradient describing the change of the material line element in the tangential surface of the reference configuration $\mathrm{d}\hat{\vec{X}} = \mathrm{d}\Theta^{\gamma} \vec{A}_{\gamma}$, i.e. the mapping $\mathrm{d}\hat{\vec{x}} = \hat{\mathbf{F}} \mathrm{d}\hat{\vec{X}}$. If both coordinates are identical, i.e. in the case of convective coordinates, $\vartheta^{\alpha} = \Theta^{\alpha}$, the in-plane deformation gradient reads $\hat{\mathbf{F}} = \vec{a}_{\alpha} \otimes \vec{A}^{\alpha}$ because $\partial \theta_{\mathrm{R}}^{\alpha} / \partial \Theta^{\beta} = \delta_{\beta}^{\alpha}$.

In order to define strains, we draw on the right Cauchy-Green tensor

$$\hat{\mathbf{C}} = \hat{\mathbf{F}}^{T} \hat{\mathbf{F}} = \theta_{\mathrm{R},\alpha}^{\gamma} \, \theta_{\mathrm{R},\beta}^{\delta} \, (\vec{A}^{\alpha} \otimes \vec{a}_{\gamma}) (\vec{a}_{\delta} \otimes \vec{A}^{\beta}) = \underbrace{\theta_{\mathrm{R},\alpha}^{\gamma} \, \theta_{\mathrm{R},\beta}^{\delta} \, a_{\gamma\delta}}_{\hat{C}_{\alpha\beta}} \vec{A}^{\alpha} \otimes \vec{A}^{\beta} = \hat{C}_{\alpha\beta} \vec{A}^{\alpha} \otimes \vec{A}^{\beta}. \tag{4}$$

In the case of convective coordinates, the coefficients of the right Cauchy-Green tensor relative to the gradient vectors (contravariant basis) are identical to the metric coefficients of the tangent vectors in the current configuration, $\hat{C}_{\alpha\beta} = a_{\alpha\beta}$. So far, the basis vectors $\vec{A}_{\alpha} \in \mathbb{V}^3$ and $\vec{A}^{\beta} \in \mathbb{V}^3$ are elements in the three-dimensional vector space. Since both vectors operate in the tangential space and form oblique-angled two-dimensional basis vectors – representing a two-dimensional space – the new basis vectors $\vec{\mathsf{A}}_{\alpha} \in \mathbb{V}^2$ should have the same norm and the same direction, $\vec{\mathsf{A}}_{\alpha} \mathrel{\hat{=}} \vec{A}_{\alpha}$. However, $\vec{\mathsf{A}}_{\alpha}$ contains only two components. This should hold for the contravariant basis as well: $\vec{\mathsf{A}}^{\beta} \in \mathbb{V}^2$, $\vec{\mathsf{A}}^{\beta} \mathrel{\hat{=}} \vec{A}^{\beta}$. Accordingly, the in-plane right Cauchy-Green tensor is represented by

$$\hat{\mathsf{C}} = \hat{C}_{\alpha\beta} \vec{\mathsf{A}}^{\alpha} \otimes \vec{\mathsf{A}}^{\beta}. \tag{5}$$

Using the contravariant metric coefficients $A^{\alpha\beta} = \vec{\mathsf{A}}^{\alpha} \cdot \vec{\mathsf{A}}^{\beta} = \vec{A}^{\alpha} \cdot \vec{A}^{\beta}$, the mixed-variant representation, $\hat{C}^{\gamma}{}_{\beta} = A^{\alpha\gamma} \hat{C}_{\alpha\beta}$, of the in-plane right Cauchy-Green tensor is obtained, $\hat{\mathsf{C}} = \hat{C}^{\gamma}{}_{\beta} \vec{\mathsf{A}}_{\gamma} \otimes \vec{\mathsf{A}}^{\beta}$, which is necessary to calculate in-plane the right stretch tensor $\hat{\mathsf{U}}$. This is achieved by determining the spectral representation of the tensor $\hat{\mathsf{C}}$. The mixed variant representation is needed to calculate the eigenvalue problem

$$[\hat{\mathsf{C}} - \mu \mathsf{I}] \vec{\mathsf{q}} = \vec{\mathsf{0}}, \tag{6}$$

i.e. in component representation

$$\left((\hat{C}^{\alpha}{}_{\gamma} - \mu \delta^{\alpha}{}_{\gamma}) \vec{\mathsf{A}}_{\alpha} \otimes \vec{\mathsf{A}}^{\gamma} \right) (q^{\beta} \vec{\mathsf{A}}_{\beta}) = [\hat{C}^{\alpha}{}_{\beta} - \mu \delta^{\alpha}{}_{\beta}] q^{\beta} \vec{\mathsf{A}}_{\alpha} = \vec{\mathsf{0}}. \tag{7}$$

This holds, due to the linear independence of the vectors $\vec{\mathsf{A}}_1$ and $\vec{\mathsf{A}}_2$, for the classical symmetric eigenvalue problem

$$\det[\hat{C}^{\alpha}{}_{\beta} - \mu \delta^{\alpha}{}_{\beta}] = \begin{vmatrix} \hat{C}^{1}{}_{1} - \mu & \hat{C}^{1}{}_{2} \\ \hat{C}^{2}{}_{1} & \hat{C}^{2}{}_{2} - \mu \end{vmatrix} = \mu^2 - \mathrm{I}_{\hat{\mathbf{C}}} \mu + \mathrm{II}_{\hat{\mathbf{C}}} = 0, \tag{8}$$

where the principal invariants (coefficients of the characteristic polynomial) read

$$\mathrm{I}_{\hat{\mathbf{C}}} = \operatorname{tr} \hat{\mathbf{C}} = \hat{\mathbf{C}} \cdot \mathbf{I} = \hat{\mathsf{C}} \cdot \mathsf{I} = \hat{C}^{1}{}_{1} + \hat{C}^{2}{}_{2} \tag{9}$$

$$\mathrm{II}_{\hat{\mathbf{C}}} = \frac{1}{2} \Big((\operatorname{tr} \hat{\mathbf{C}})^2 - \operatorname{tr} \hat{\mathbf{C}}^2 \Big) = \frac{1}{2} \Big((\operatorname{tr} \hat{\mathsf{C}})^2 - \operatorname{tr} \hat{\mathsf{C}}^2 \Big) = \det[\hat{C}^{\alpha}{}_{\beta}] = \hat{C}^{1}{}_{1} \hat{C}^{2}{}_{2} - \hat{C}^{1}{}_{2} \hat{C}^{2}{}_{1}, \tag{10}$$

but $\mathrm{III}_{\hat{\mathbf{C}}} = \det \hat{\mathbf{C}} = 0$. The solution of Eq.(8) is given by

$$\mu_{1,2} = \frac{\mathrm{I}_{\hat{\mathbf{C}}}}{2} \pm \sqrt{\frac{\mathrm{I}_{\hat{\mathbf{C}}}^2}{4} - \mathrm{II}_{\hat{\mathbf{C}}}^2}. \tag{11}$$

Here, we apply a numerical eigenvalue and eigenvector computation. The eigensolver provides the coefficients of the eigenvectors,

$$\mathbf{q}_1 = \left\{ \begin{array}{c} {q^1}_1 \\ {q^2}_1 \end{array} \right\}, \qquad \mathbf{q}_2 = \left\{ \begin{array}{c} {q^1}_2 \\ {q^2}_2 \end{array} \right\}, \tag{12}$$

i.e. the eigenvectors $\vec{\mathsf{q}}$ relative to the oblique-angled read

$$\vec{\mathsf{q}}_1 = {q^\alpha}_1 \vec{\mathsf{A}}_\alpha \quad \text{and} \quad \vec{\mathsf{q}}_2 = {q^\alpha}_2 \vec{\mathsf{A}}_\alpha, \tag{13}$$

where the eigenvectors are orthogonal, $\vec{\mathsf{q}}_1 \cdot \vec{\mathsf{q}}_2 = 0$ but not $\vec{\mathsf{A}}_\alpha \cdot \vec{\mathsf{A}}_\beta = A_{\alpha\beta}$. The eigenvectors are chosen to be normalized in the following, $\vec{\mathsf{n}}_\alpha = \vec{\mathsf{q}}_\alpha / |\vec{\mathsf{q}}_\alpha|$ and to be right-handed and orthogonal, $\vec{\mathsf{n}}_\alpha \cdot \vec{\mathsf{n}}_\beta = \delta_{\alpha\beta}$, so that the spectral representation of the right Cauchy-Green tensor reads

$$\hat{\mathsf{C}} = \sum_{\alpha=1}^{2} \mu_\alpha \vec{\mathsf{n}}_\alpha \otimes \vec{\mathsf{n}}_\alpha. \tag{14}$$

In view of the definition of strain tensors, the polar decomposition of the deformation gradient $\hat{\mathbf{F}} = \hat{\mathbf{R}}\hat{\mathbf{U}}$ or $\hat{\mathsf{F}} = \hat{\mathsf{R}}\hat{\mathsf{U}}$ is applied. $\hat{\mathsf{R}}^{-1} = \hat{\mathsf{R}}^T$, with $\det \hat{\mathsf{R}} = +1$, is a pure rotation within the tangential space, and $\hat{\mathsf{U}} = \hat{\mathsf{U}}^T$ is a positive definite and symmetric tensor (which is not true for $\hat{\mathbf{U}}$). The latter represents the right stretch tensor in the tangential space describing the stretch of the material line elements $\mathrm{d}\hat{\vec{X}}$. Now, the stretch tensor can be computed by

$$\hat{\mathsf{U}} = \hat{\mathsf{C}}^{1/2} = \sum_{\alpha=1}^{2} \mu_\alpha^{1/2} \vec{\mathsf{n}}_\alpha \otimes \vec{\mathsf{n}}_\alpha = \sum_{\alpha=1}^{2} \lambda_\alpha \vec{\mathsf{n}}_\alpha \otimes \vec{\mathsf{n}}_\alpha. \tag{15}$$

$\lambda_\alpha = \mu_\alpha^{1/2}$ are the eigenvalues and $\vec{\mathsf{n}}_\alpha \in \mathbb{V}^2$ the eigenvectors of the in-plane right stretch tensor $\hat{\mathsf{U}}$, which can be provided relative to the original basis

$$\hat{\mathsf{U}} = \sum_{\alpha=1}^{2} \lambda_\alpha \vec{\mathsf{n}}_\alpha \otimes \vec{\mathsf{n}}_\alpha = \underbrace{\sum_{\alpha=1}^{2} \frac{\lambda_\alpha}{|\vec{\mathsf{q}}_\alpha|^2} {q^\beta}_\alpha {q^\gamma}_\alpha}_{\hat{U}^{\beta\gamma}} \vec{\mathsf{A}}_\beta \otimes \vec{\mathsf{A}}_\gamma, \tag{16}$$

with $|\vec{\mathsf{q}}_\alpha| = \sqrt{{q^\beta}_\alpha \vec{\mathsf{A}}_\beta \cdot {q^\gamma}_\alpha \vec{\mathsf{A}}_\gamma} = \sqrt{{q^\beta}_\alpha {q^\gamma}_\alpha A_{\beta\gamma}}$, $\not\Sigma \alpha$. Since $\vec{\mathsf{A}}_\alpha$ contains only the information of the direction and has a norm, it is not explicitly provided with numbers (such as a column vector in linear algebra). Moreover, $\vec{\mathsf{A}}_\alpha$ are oblique-angled vectors in the general case. Thus, the matrix representation of the surface right stretch tensor $\hat{\mathsf{U}}$ has only the meaning relative to the basis $\vec{\mathsf{A}}_1$ and $\vec{\mathsf{A}}_2$, which is not helpful in the case of curvilinear coordinates. The only case in which the coefficients in $\hat{\mathsf{U}}$ can be directly interpreted with stretches in the global coordinate system is for Cartesian coordinates in the reference configuration. If there is an out-of-plane component in the tangent vectors $\vec{A}_\alpha$ this does not hold anymore.

Moreover, $\hat{U}^{\beta\gamma}$ are no physical coordinates because the basis vectors $\vec{\mathsf{A}}_\beta$ are not necessarily unit vectors. Nevertheless, it is possible to assign an in-plane stretch tensor $\hat{\mathbf{U}}$ relative to the tangential space

$$\hat{\mathbf{U}} = \sum_{\alpha=1}^{2} \frac{\lambda_\alpha}{|\vec{\mathsf{q}}_\alpha|^2} q^\beta{}_\alpha q^\gamma{}_\alpha \vec{A}_\beta \otimes \vec{A}_\gamma \tag{17}$$

and general strain tensors defined by the principal strains

$$\epsilon_\alpha^{(\mathrm{m})} = \begin{cases} \dfrac{1}{m}(\lambda_\alpha^m - 1) & \text{if } m \neq 0 \\ \ln \lambda_\alpha & \text{if } m = 0 \end{cases} \tag{18}$$

(Seth-Hill strain measure). As is well-known, these strains have the property of vanishing in the undeformed state $\epsilon_\alpha^{(\mathrm{m})}|_{\lambda_\alpha=1} = 0$ and to be monotonous increasing, $\partial\epsilon_\alpha^{(\mathrm{m})}/\partial\lambda_\alpha > 0$ for $\lambda_\alpha > 0$. Moreover, all principal strains coincide in the undeformed state, $\partial\epsilon_\alpha^{(\mathrm{m})}/\partial\lambda_\alpha|_{\lambda_\alpha=1} = 1$. Accordingly, we obtain the representation of generalized strain tensors

$$\hat{\mathsf{E}}^{(\mathrm{m})} = \sum_{\alpha=1}^{2} \epsilon_\alpha^{(\mathrm{m})} \vec{\mathsf{n}}_\alpha \otimes \vec{\mathsf{n}}_\alpha, \tag{19}$$

see, for example, [8, 9]. Commonly, only the values $m = 0, 1, 2$ are chosen, i.e. for the tensors in the tangential surface we have

$$\hat{\mathsf{E}}^{(0)} = \ln \hat{\mathsf{U}}, \qquad \hat{\mathsf{E}}^{(1)} = \hat{\mathsf{U}} - \hat{\mathsf{I}}, \qquad \hat{\mathsf{E}}^{(2)} = \frac{1}{2}(\hat{\mathsf{C}} - \hat{\mathsf{I}}). \tag{20}$$

The first tensor is called Hencky-strain tensor and the third one defines the Green(-Lagrange) strain tensor, here relative to the tangential space. The component representation is relative to the tangential or relative to the three-dimensional space, respectively,

$$\hat{\mathsf{E}}^{(m)} = \sum_{\alpha=1}^{2} \frac{\epsilon_\alpha^{(m)}}{|\vec{\mathsf{q}}_\alpha|^2} q^\beta{}_\alpha q^\gamma{}_\alpha \vec{\mathsf{A}}_\beta \otimes \vec{\mathsf{A}}_\gamma, \quad \hat{\mathbf{E}}^{(m)} = \sum_{\alpha=1}^{2} \frac{\epsilon_\alpha^{(m)}}{|\vec{\mathsf{q}}_\alpha|^2} q^\beta{}_\alpha q^\gamma{}_\alpha \vec{A}_\beta \otimes \vec{A}_\gamma. \tag{21}$$

The DIC-system provides a number of points (coordinates) in the initial and the current configuration, where a subset of points is chosen for the surface description. Either one takes a least-square method and fits the points by an interpolation function, or one can follow a description as applied in finite elements. We follow the second proposal and assume the coordinate representation

$$\mathbf{X}(\Theta^1, \Theta^2) = \sum_{k=1}^{n_{\mathrm{en}}} N_k(\Theta^1, \Theta^2) \mathbf{X}_k \quad \Rightarrow \quad \vec{X}(\Theta^1, \Theta^2) = \left(\sum_{k=1}^{n_{\mathrm{en}}} N_k(\Theta^1, \Theta^2) X_{kj} \right) \vec{e}_j \tag{22}$$

with the shape functions $N_k(\Theta^1, \Theta^2)$, $k = 1, \ldots, n_{\mathrm{en}}$, see, in view of the (shape-)functions $N_k(\Theta^1, \Theta^2)$, for example, [10], where $\mathbf{X}_k$ are the coordinates of a subset of DIC-points in the reference state. Choosing the same ansatz for the coordinates in the current configuration

$$\mathbf{x}(\Theta^1, \Theta^2) = \sum_{k=1}^{n_{\mathrm{en}}} N_k(\Theta^1, \Theta^2) \mathbf{x}_k, \quad \Rightarrow \quad \vec{x}(\Theta^1, \Theta^2) = \left(\sum_{k=1}^{n_{\mathrm{en}}} N_k(\Theta^1, \Theta^2) x_{kj} \right) \vec{e}_j \tag{23}$$

leads to the case of convective coordinates. Here, $\mathbf{x}_k$, $k = 1, \ldots, n_{\text{en}}$, define the coordinates of the measured points in the current state. Accordingly, at every point of the pattern the strains can be calculated using formula (21). Another possibility would be to apply smoothing techniques such as the mean-value determination at each node, drawing on the connecting pattern information. For a given unknown and an irregular cloud of points a triangulation can be chosen, see, for example, [11, 12]. In a triangle, see [13] for a similar approach, a constant stretch occurs. Here, we have to decide at each node which stretch has to be chosen, or whether to compute the mean-value of the patterns connected to that node. Our examples are based on the latter. A nine-noded approach focuses – quite naturally – on a curvilinear surface description, whereas the triangulation is, a priori, in the tangential space.

3 Finite Element Validation

As discussed in detail in the introduction, the displacement and strain determination on the surface of a finite element mesh is of particular interest. The strain determination of Section 2 can be used either for the DIC-system or for the finite element surface, due to the fact that both cases involve a given cloud of points. In order to compare both results, we start off by discussing the projection technique, i.e. the projection of the DIC-data onto the finite element mesh. Afterwards, an example is chosen to demonstrate the behavior and the applicability of the procedure.

3.1 Projection of Data

We assume a configuration at time t in the DIC-system and the finite element simulation, see Fig. 2. The time t should be identical in both analyses, but the DIC-system and the FE-

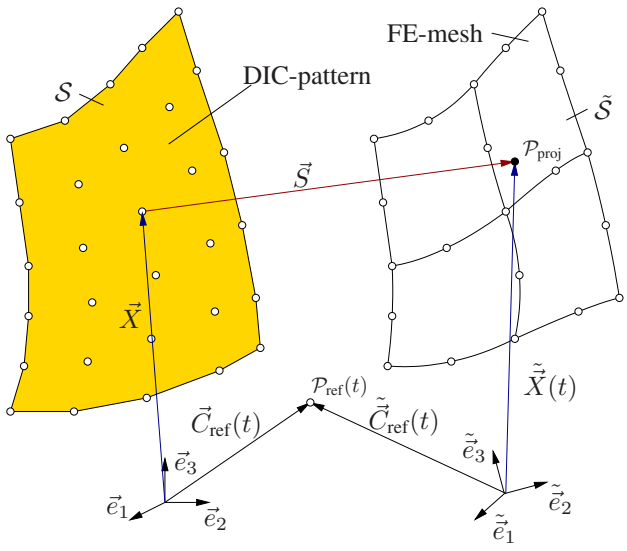

Figure 2: Geometrical problem (as an example elements with 8 nodes at the surface are assumed, which might be surface nodes of 20-noded hexahedral elements)

program can have different coordinate systems. Here, we assume that both are of Cartesian-type. They must be related by a known change of basis. If $\vec{e}_k$, $k = 1, 2, 3$, is the coordinate system of the DIC-system and $\tilde{\vec{e}}_k$, $k = 1, 2, 3$, the basis of the FE-program, they are related by

$$\tilde{\vec{e}}_i = Q_{ji}\vec{e}_j, \quad \text{with} \quad Q_{ij} = \vec{e}_i \cdot \tilde{\vec{e}}_j. \tag{24}$$

In the following, all quantities with a tilde indicate the finite element solution, while values without a specific symbol represent the DIC-response. For a real comparison, a point $\mathcal{P}_{\text{ref}}(t)$ must be known which is the same in both systems (possibly the clamp for fixing the specimen or a point chosen by the user). In the following calculations, both the matrix $\mathbf{Q} = [Q_{ij}] \in \mathbb{R}^{3\times3}$ as well as the motion of the reference point $\vec{C}_{\text{ref}}(t)$ and $\tilde{\vec{C}}_{\text{ref}}(t)$ must be known. Since both surfaces are not exactly the same, we have to project a point of the DIC-system onto the surface of the FE-mesh, i.e. the vector $\vec{S}$ is perpendicular to the surface of the FE-mesh and its norm obtains a minimum. Of course, it is also possible to proceed in the opposite way, i.e. to project onto the surface description of the DIC-system. However, if one has no access to the surface description of the DIC-system, the projection onto a finite element is much easier, because the shape-functions are well-known. The surface of the FE-mesh is obtained only by the coordinates of the elements, the nodal incidences of all elements, and the node numbers on the surface.

Let $\vec{X} \in \mathcal{S}$ be the vector of a material point in the DIC-system and $\tilde{\vec{X}} \in \tilde{\mathcal{S}}$ the projected point in the finite element surface, both in the initial configuration. We look for the vector

$$\vec{S}(\tilde{\Theta}^1, \tilde{\Theta}^2) = \vec{X} - \vec{C}_{\text{ref}} - (\tilde{\vec{X}}(\tilde{\Theta}^1, \tilde{\Theta}^2) - \tilde{\vec{C}}_{\text{ref}}) \tag{25}$$

so that the norm of the projection vector becomes a minimum

$$\|\vec{S}(\tilde{\Theta}^1, \tilde{\Theta}^2)\| \to \text{min.} \tag{26}$$

see Fig. 2. Eq.(26) leads to two non-linear equations

$$\frac{\partial \tilde{\vec{X}}(\tilde{\Theta}^1, \tilde{\Theta}^2)}{\partial \tilde{\Theta}^\alpha} \cdot \vec{S}(\tilde{\Theta}^1, \tilde{\Theta}^2)\Big|_{\tilde{\Theta}^\alpha = \tilde{\Theta}^\alpha_{\text{proj}}} = 0, \quad \alpha = 1, 2 \tag{27}$$

to calculate the coordinates $\tilde{\Theta}^\alpha_{\text{proj}}$ in the finite element mesh. One major task is to find the element where the pattern point $\vec{X}$ is mapped on. This is done in a straight-forward manner by searching the element and the coordinates $\tilde{\Theta}^\alpha_{\text{proj}}$ within a loop over the number of DIC-points.

3.2 Validation Example

For the following example, we carried out a tensile test of a plane specimen with a hole, see Fig. 3(a). The geometry of the specimen is shown in Fig. 3(a). The material under consideration is a PP/PE foil of 0.6mm thickness. The displacement of the testing machine's traverse is chosen to be 2mm. Spray-paint was applied to the surface in such a way that the GOM-system, see [14], could identify the spray pattern, see Fig. 3(a). Additionally, some

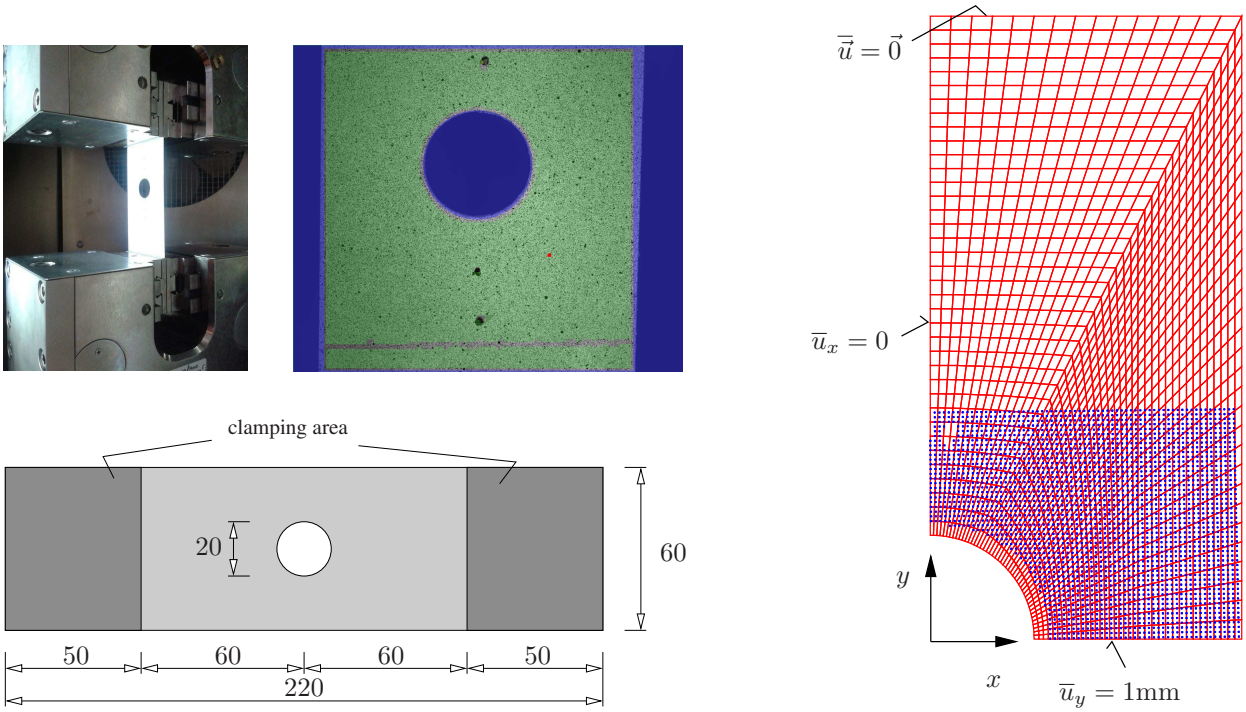

(a) Plate with a hole and pattern on the specimen as well as its geometry (thickness 0.6 mm)

(b) Mesh of the surface and DIC-pattern in the reference configuration

Figure 3: Geometry and element mesh of a quarter enriched with DIC-pattern

auxiliary points were painted onto the surface, which are not evaluated in the following investigations.

In order to compare the experimental observation with a finite element solution, we exploit the symmetry conditions and consider only one quarter of the specimen, see Fig. 3(b), which is common in finite elements. In thickness direction, two three-dimensional elements are used (element-type C3D8R of the commercial finite element program Abaqus, [15]). The symmetry conditions are zero-displacements in x-direction on the left-hand side and a displacement of 1mm in y-direction at the bottom. All displacements are fixed at the top to model the clamps of the testing machine. The GOM-system measures the major and minor logarithmic strains, see Eq.(18)$_1$ for $\alpha = 1, 2$. Figs. 4 show the results of the logarithmic strains, where the maximum lies at approximately 5% at the horizontal point of the circular hole. The computations were done with a Neo-Hookean model ($c_{10} = 7.28\text{MPa}$ and $D_1 = 1.4 \times 10^{-3}\text{MPa}^{-1}$). Since the main focus lies on the procedure, the constitutive model is of minor importance in this article. Fig. 5 shows Abaqus results for the entire quarter at the surface of the brick-elements. Here, we have $\mathbf{Q} = \mathbf{I}$, $\vec{C}_{\text{ref}} = 28\vec{e}_1\text{mm}$ and $\tilde{\vec{C}}_{\text{ref}} = \vec{0}$, see Eq.(24) and Fig. 2.

Using the projection of Section 3.1 with the strain determination scheme of Section 2, the displacement and maximum principal strain difference at the k-th point

$$\Delta u_{xk} = \tilde{u}_{xk} - u_{xk} \quad \text{and} \quad \Delta \epsilon^{(0)}_{\text{max}\,k} = \tilde{\epsilon}_{\text{max}\,k} - \epsilon_{\text{max}\,k} \tag{28}$$

are exemplarily shown in Fig. 6. The strains are more sensitive and scattered than it is known for finite elements. Thus, a tool is available for both model validation and material parameter identification.

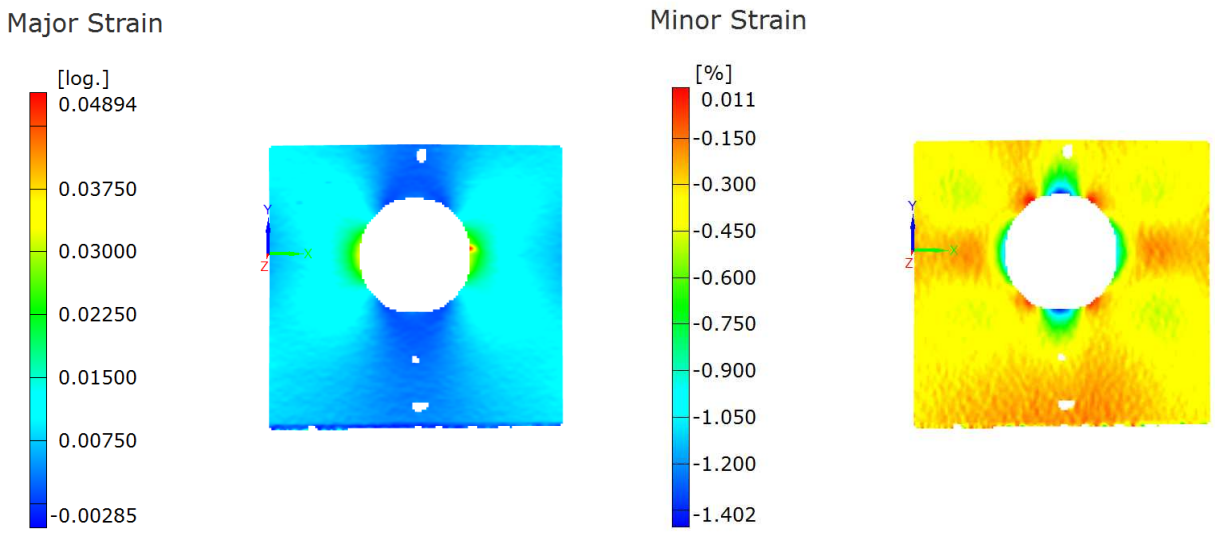

(a) Maximum logarithmic strains (b) Minimum technical strains

Figure 4: Result of GOM-system for maximum and minimum logarithmic strains

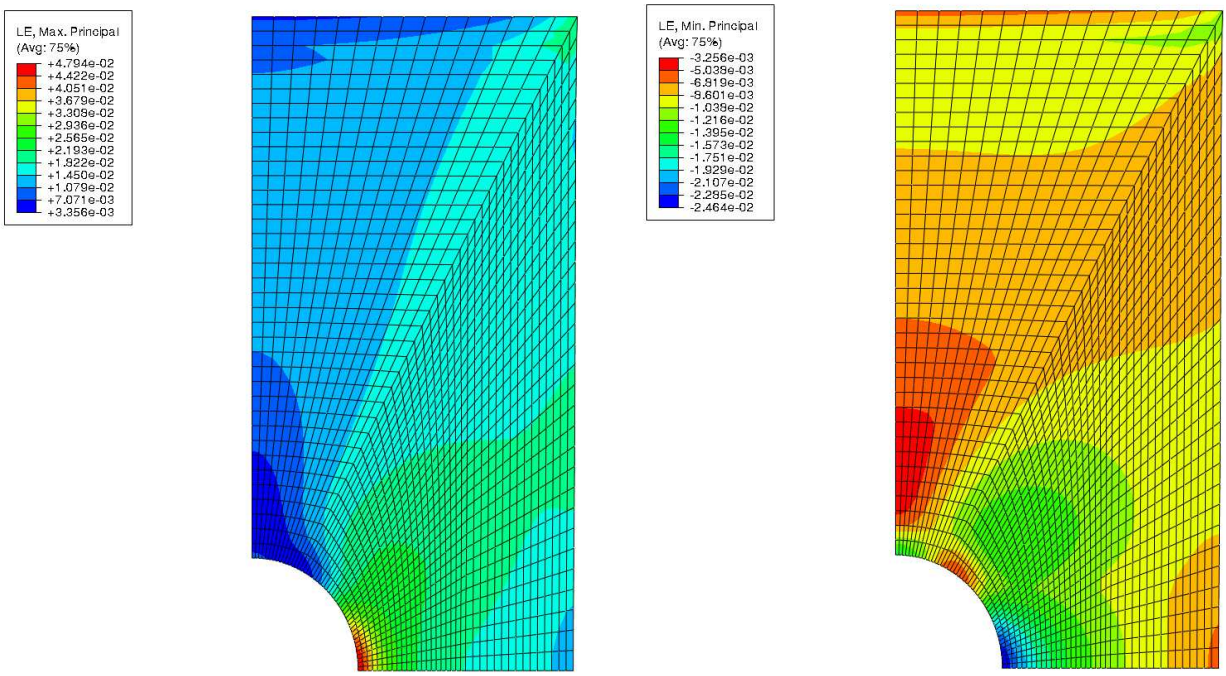

(a) Maximum logarithmic strains (b) Minimum logarithmic strains

Figure 5: Strain result of Abaqus for a quarter of the specimen

References

[1] M. A. Sutton, J.-J. Orteu, and H.-W. Schreier. *Image correlation for shape, motion and deformation measurements*. Springer, New York, 2009.

[2] M. E. Gurtin and A. I. Murdoch. A continuum theory of elastic material surfaces.

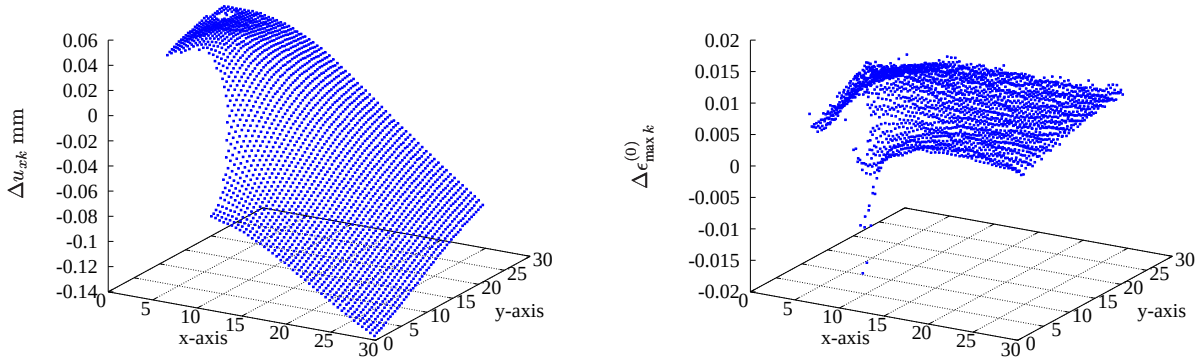

(a) Difference in displacement in horizontal x-direction

(b) Difference in maximum logarithmic strains

Figure 6: Difference between DIC-system and Abaqus solution evaluated at the referential coordinates of the DIC-system

Archive of Rational Mechanics and Analysis, 57:291–323, 1975.

[3] A. Papastavrou, P. Steinmann, and E. Kuhl. In the mechanics of continua with boundary energies and growing surfaces. *Journal of the Mechanics and Physics of Solids*, 61:1446–1463, 2013.

[4] A. Javili, A. McBride, and P. Steinmann. Thermomechanics of solids with lower-dimensional energetics: on the importance of surface, interface and curve structures at the nanoscale. A unifying review. *Applied Mechanics Review*, 65(1):1–31, 2013.

[5] C. Truesdell and R. Toupin. *Principles of classical mechanics and field theory*, volume III/1 of *Encyclopedia of Physics*, chapter The classical field theories, pages 226 – 793. Springer, Berlin – Göttingen – Heidelberg, 1960.

[6] Y. Basar and W. B. Krätzig. *Mechanik der Flächentragwerke*. Vieweg, Braunschweig, 1985.

[7] S. Hartmann. Computational aspects of the symmetric eigenvalue problem of second order tensors. *Technische Mechanik*, 23(2-4):283–294, 2003.

[8] R. W. Ogden. *Non-Linear Elastic Deformations*. Ellis Horwood, Chichester, 1984.

[9] P. Haupt and C. Tsakmakis. Stress tensors associated with deformation tensors via duality. *Archive of Mechanics*, 48:347–384, 1996.

[10] T. J. R. Hughes. *The finite element method*. Prentice-Hall, Engelwood Cliffs, New Jersey, 1st edition, 1987.

[11] J. R. Shewchuk. Triangle: Engineering a 2D Quality Mesh Generator and Delaunay Triangulator. In Ming C. Lin and Dinesh Manocha, editors, *Applied Computational Geometry: Towards Geometric Engineering*, volume 1148 of *Lecture Notes in Computer Science*, pages 203–222. Springer-Verlag, 1996. From the First ACM Workshop on Applied Computational Geometry.

[12] J. R. Shewchuk. Delaunay refinement algorithms for triangular mesh generation. *Computational Geometry: Theory and Applications*, 22(1-3):21–74, 2002.

[13] F. P. K. Hsu, C. Schwab, D. Rigamonti, and J. D. Humphrey. Identification of response functions from axisymmetric membrane inflation tests: implications for biomechanics. *International Journal of Solids and Structures*, 31:3375–3386, 1994.

[14] GOM. *Aramis – User Manual: The basics of strain*. GOM – Gesellschaft für optische Messtechnik, Braunschweig, Germany, 2011.

[15] Abaqus. Abaqus 6.12 documentation. `www.3ds.com/products-services/simulia/portfolio/abaqus/overview/`, 2012.

Author's Address:

Prof. Dr.-Ing. Stefan Hartmann
Dr.-Ing. Carmen Sguazzo

Clausthal University of Technology
Institute of Applied Mechanics
Adolph-Roemer-Str. 2a
38678 Clausthal-Zellerfeld
Germany

E-Mail: stefan.hartmann@tu-clausthal.de